Electronic Supplementary Material (ESI) for RSC Advances.
This journal is © The Royal Society of Chemistry 2016

Supporting Information

Quantum Chemical Calculations with AIM Approach for the π-Interactions between Hydrogen Chalcogenides and Naphthalene

Satoko Hayashi,* Yuji Sugibayashi and Waro Nakanishi*

Department of Material Science and Chemistry, Faculty of Systems Engineering, Wakayama University, 930 Sakaedani, Wakayama, 640-8510 Japan
E-mail: hayashi3@sys.wakayama-u.ac.jp and nakanisi@sys.wakayama-u.ac.jp

QTAIM Dual Functional Analysis (QTAIM-DFA)

The bond critical point (BCP; ∗) is an important concept in QTAIM. The BCP of $(\omega, \sigma) = (3, -1)$[S1] is a point along the bond path (BP) at the interatomic surface, where charge density $\rho(\boldsymbol{r})$ reaches a minimum. It is donated by $\rho_b(\boldsymbol{r}_c)$. While the chemical bonds or interactions between A and B are denoted by A–B, which correspond to BPs between A and B in QTAIM, A-∗-B emphasizes the presence of BCP (∗) in A–B.

The sign of the Laplacian $\rho_b(\boldsymbol{r}_c)$ ($\nabla^2\rho_b(\boldsymbol{r}_c)$) indicates that $\rho_b(\boldsymbol{r}_c)$ is depleted or concentrated with respect to its surrounding, since $\nabla^2\rho_b(\boldsymbol{r}_c)$ is the second derivative of $\rho_b(\boldsymbol{r}_c)$. $\rho_b(\boldsymbol{r}_c)$ is locally depleted relative to the average distribution around $\boldsymbol{r}_c$ if $\nabla^2\rho_b(\boldsymbol{r}_c) > 0$, but it is concentrated when $\nabla^2\rho_b(\boldsymbol{r}_c) < 0$. Total electron energy densities at BCPs ($H_b(\boldsymbol{r}_c)$) must be a more appropriate measure for weak interactions on the energy basis.[S1-S6] $H_b(\boldsymbol{r}_c)$ are the sum of kinetic energy densities ($G_b(\boldsymbol{r}_c)$) and potential energy densities ($V_b(\boldsymbol{r}_c)$) at BCPs, as shown in eq (S1). Electrons at BCPs are stabilized when $H_b(\boldsymbol{r}_c) < 0$, therefore, interactions exhibit the covalent nature in this region, whereas they exhibit no covalency if $H_b(\boldsymbol{r}_c) > 0$, due to the destabilization of electrons at BCPs under the conditions.[S1] Eq (S2) represents the relation between $\nabla^2\rho_b(\boldsymbol{r}_c)$ and $H_b(\boldsymbol{r}_c)$, together with $G_b(\boldsymbol{r}_c)$ and $V_b(\boldsymbol{r}_c)$, which is closely related to the virial theorem.

$$H_b(\boldsymbol{r}_c) = G_b(\boldsymbol{r}_c) + V_b(\boldsymbol{r}_c) \quad \text{(S1)}$$

$$(\hbar^2/8m)\nabla^2\rho_b(\boldsymbol{r}_c) = H_b(\boldsymbol{r}_c) - V_b(\boldsymbol{r}_c)/2 \quad \text{(S2)}$$

$$= G_b(\boldsymbol{r}_c) + V_b(\boldsymbol{r}_c)/2 \quad \text{(S2')}$$

Interactions are classified by the signs of $\nabla^2\rho_b(\boldsymbol{r}_c)$ and $H_b(\boldsymbol{r}_c)$. Interactions in the region of $\nabla^2\rho_b(\boldsymbol{r}_c) < 0$ are called shared-shell (SS) interactions and they are closed-shell (CS) interactions for $\nabla^2\rho_b(\boldsymbol{r}_c) > 0$. $H_b(\boldsymbol{r}_c)$ must be negative when $\nabla^2\rho_b(\boldsymbol{r}_c) < 0$, since $H_b(\boldsymbol{r}_c)$ are larger than $(\hbar^2/8m)\nabla^2\rho_b(\boldsymbol{r}_c)$ by $V_b(\boldsymbol{r}_c)/2$ with negative $V_b(\boldsymbol{r}_c)$ at all BCPs (eq (S2)). Consequently, $\nabla^2\rho_b(\boldsymbol{r}_c) < 0$ and $H_b(\boldsymbol{r}_c) < 0$ for the SS interactions. The CS interactions are especially called *pure* CS interactions for $H_b(\boldsymbol{r}_c) > 0$ and $\nabla^2\rho_b(\boldsymbol{r}_c) > 0$, since electrons at BCPs are depleted and destabilized under the conditions.[S1a] Electrons in the intermediate region between SS and *pure* CS, which belong to CS, are locally depleted but stabilized at BCPs, since $\nabla^2\rho_b(\boldsymbol{r}_c) > 0$ but $H_b(\boldsymbol{r}_c) < 0$.[S1a] We call the interactions in this region *regular* CS,[S4,S5] when it is necessary to distinguish

from *pure* CS. The CT interactions belong to the *regular* CS region, where the orbital overlaps become to play an important role, while the overlaps do not so in the *regular* CS region. The role of $\nabla^2\rho_b(\boldsymbol{r}_c)$ in the classification can be replaced by $H_b(\boldsymbol{r}_c) - V_b(\boldsymbol{r}_c)/2$, since $(\hbar^2/8m)\nabla^2\rho_b(\boldsymbol{r}_c) = H_b(\boldsymbol{r}_c) - V_b(\boldsymbol{r}_c)/2$ (eq (S2)).

We proposed QTAIM-DFA by plotting $H_b(\boldsymbol{r}_c)$ versus $H_b(\boldsymbol{r}_c) - V_b(\boldsymbol{r}_c)/2$ $(= (\hbar^2/8m)\nabla^2\rho_b(\boldsymbol{r}_c))$,[S4a] after the proposal of $H_b(\boldsymbol{r}_c)$ versus $\nabla^2\rho_b(\boldsymbol{r}_c)$.[S4b] Both axes in the plot of the former are given in energy unit, therefore, distances on the (x, y) $(= (H_b(\boldsymbol{r}_c) - V_b(\boldsymbol{r}_c)/2, H_b(\boldsymbol{r}_c))$ plane can be expressed in the energy unit, which provides an analytical development. QTAIM-DFA can incorporate the classification of interactions by the signs of $\nabla^2\rho_b(\boldsymbol{r}_c)$ and $H_b(\boldsymbol{r}_c)$. Scheme S1 summarizes the QTAIM-DFA treatment. Interactions of *pure* CS appear in the first quadrant, those of *regular* CS in the forth quadrant and SS interactions do in the third quadrant. No interactions appear in the second one.

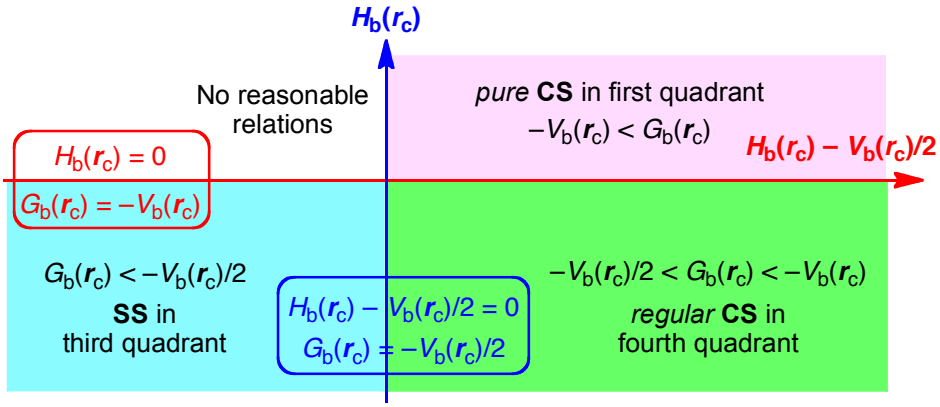

Scheme S1. QTAIM-DFA: Plot of $H_b(\boldsymbol{r}_c)$ versus $H_b(\boldsymbol{r}_c) - V_b(\boldsymbol{r}_c)/2$ for Weak to Strong Interactions

In our treatment, data for perturbed structures around fully optimized structures are also employed for the plots, together with the fully optimized ones (see Figure S1).[S4-S6] We proposed the concept of the "dynamic nature of interaction" originated from the perturbed structures. The behavior of interactions at the fully optimized structures corresponds to "the static nature of interactions", whereas that containing perturbed structures exhibit the "dynamic nature of interaction" as explained below. The method to generate the perturbed structures is discussed later. Plots of $H_b(\boldsymbol{r}_c)$ versus $H_b(\boldsymbol{r}_c) - V_b(\boldsymbol{r}_c)/2$ are analyzed employing the polar coordinate (R, θ) representation with (θ_p, κ_p) parameters.[S4a,S5,S6] Figure S1 explains the treatment. R in (R, θ) is defined by eq (S3) and given in the energy unit. R corresponds to the energy for an interaction at BCP. The plots show a spiral stream, as a whole. θ in (R, θ) defined by eq (S4), measured from the y-axis, controls the spiral stream of the plot. Each plot for an interaction shows a specific curve, which provides important information of the interaction (see Figure S1). The curve is expressed by θ_p and κ_p. While θ_p, defined by eq (S5) and measured from the y-direction, corresponds to the tangent line of a plot, where θ_p is calculated employing data of the perturbed structures with a fully-optimized structure and κ_p is the curvature of the plot (eq (S6)). While (R, θ) correspond to the static nature, (θ_p, κ_p) represent the dynamic nature of interactions. We call (R, θ) and (θ_p, κ_p) QTAIM-DFA parameters, whereas $\rho_b(\boldsymbol{r}_c)$, $\nabla^2\rho_b(\boldsymbol{r}_c)$, $G_b(\boldsymbol{r}_c)$, $V_b(\boldsymbol{r}_c)$, $H_b(\boldsymbol{r}_c)$, and $H_b(\boldsymbol{r}_c) - V_b(\boldsymbol{r}_c)/2$ belong to QTAIM functions. $k_b(\boldsymbol{r}_c)$, defined by eq (S7), is an QTAIM function but it will be treated as if it were an QTAIM-DFA parameter, if suitable.

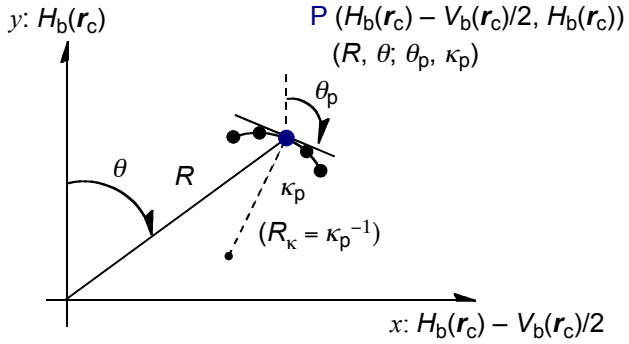

Fig. S1 Polar (R, θ) coordinate representation of $H_b(\boldsymbol{r}_c)$ versus $H_b(\boldsymbol{r}_c) - V_b(\boldsymbol{r}_c)/2$, with ($\theta_p$, κ_p) parameters.

$$R = (x^2 + y^2)^{1/2} \tag{S3}$$

$$\theta = 90^\circ - \tan^{-1}(y/x) \tag{S4}$$

$$\theta_p = 90^\circ - \tan^{-1}(dy/dx) \tag{S5}$$

$$\kappa_p = |d^2y/dx^2| / [1 + (dy/dx)^2]^{3/2} \tag{S6}$$

$$k_b(\boldsymbol{r}_c) = V_b(\boldsymbol{r}_c)/G_b(\boldsymbol{r}_c) \tag{S7}$$

where $(x, y) = (H_b(\boldsymbol{r}_c) - V_b(\boldsymbol{r}_c)/2, H_b(\boldsymbol{r}_c))$

Criteria for Classification of Interactions: Behavior of Typical Interactions Elucidated by QTAIM-DFA

$H_b(\boldsymbol{r}_c)$ are plotted versus $H_b(\boldsymbol{r}_c) - V_b(\boldsymbol{r}_c)/2$ for typical interactions in vdW (van der Waals interactions), HB (hydrogen bonds), CT-MC (molecular complexes through charge transfer), X_3^- (trihalide ions), CT-TBP (trigonal bipyramidal adducts through charge-transfer), Cov-w (weak covalent bonds), and Cov-s (strong covalent bonds).[S4-S6] Rough criteria are obtained, after the analysis of the plots for the typical interactions according to eqs (S3)–(S7), by applying QTAIM-DFA. Scheme S2 shows the rough criteria, which are accomplished by the θ and θ_p values, together with the values of $k_b(\boldsymbol{r}_c)$. The criteria will be employed to discuss the nature of interactions in question, as a reference.

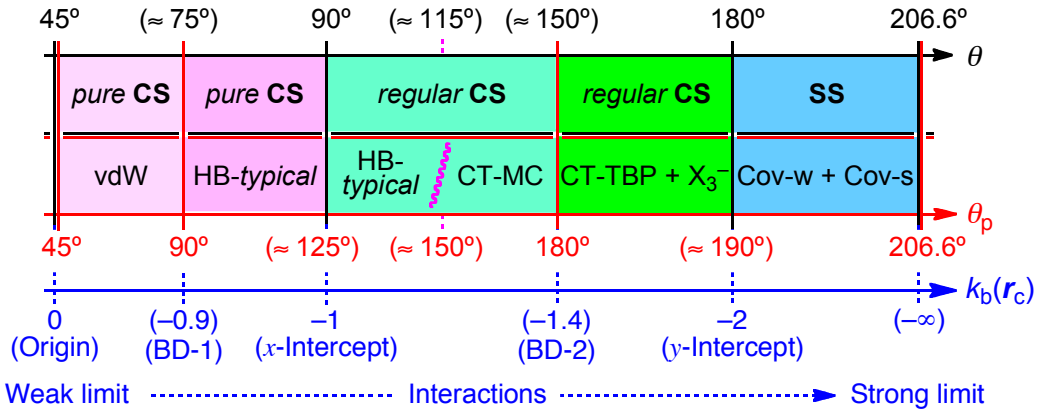

Scheme S2. Rough classification of interactions by θ and θ_p, together with $k_b(\boldsymbol{r}_c)$ (= $V_b(\boldsymbol{r}_c)/G_b(\boldsymbol{r}_c)$).

Methodological Details in Calculations

Structures were optimized employing the Gaussian 09 program.[S7] Several types of basis set systems (BSSs: BSS-A, BSS-B, BSS-C, BSS-D, BSS-E and BSS-F) were examined for the evaluation. Table S1 summarizes the BSSs. The basis set for Te of the 6-311G* type[S8] was obtained from EMSL Basis Set Exchange Library.[S9,S10] Higher basis set for Te of the (7433111/743111/7411/2 + 1s1p1d1f) type was from Sapporo Basis Set Factory.[S11] The diffusion functions of the *sp* parts for Te in (7433111/743111/7411/2 + 1s1p1d1f)[S12] were diverted as those of the *sp* type for the 6-311G* basis set of Te, since the diffusion functions could not be found for 6-311G* of Te. The Møller-Plesset second order energy correlation (MP2) level is applied to the calculations.[S13] The optimized structures were confirmed by the frequency analysis. The abbreviated notation of MP2/BSS-X (X = A, B, C, D, E and F) will also be used to describe the calculation methods employing BSS-X at the MP2 level, if suitable.

Table S1 Basis set systems employed for the calculations

Method	C, H	O, S, and Se	Te
BSS-C	6-311G(d, p)	6-311G(3d)	(7433111/743111/7411/2 + 1s1p1d1f)[a]
BSS-D	6-311G(d, p)	6-311G(3df)	(7433111/743111/7411/2 + 1s1p1d1f)[a]
BSS-E	6-311G(d, p)	6-311+G(3df)	(7433111/743111/7411/2 + 1s1p1d1f)[a]
BSS-F	6-311++G(d, p)	6-311+G(3df)	(7433111/743111/7411/2 + 1s1p1d1f)[a]

[a] The higher basis set of the (7433211/743111/7411/2 + 1s1p1d1f) type for Te was obtained from Sapporo Basis Set Factory.[S5]

References

(S1) (a) *Atoms in Molecules. A Quantum Theory*: R. F. W. Bader, Ed. Oxford University Press, Oxford, UK, **1990**. (b) C. F. Matta and R. J. Boyd, *An Introduction to the Quantum Theory of Atoms in Molecules* in *The Quantum Theory of Atoms in Molecules: From Solid State to DNA and Drug Design*: C. F. Matta and R. J. Boyd, Eds., WILEY-VCH, Weinheim, Germany, **2007**, Chap. 1.

(S2) (a) R. F. W. Bader, T. S. Slee. D. Cremer and E. Kraka, *J. Am. Chem. Soc.* **1983**, *105*, 5061–5068. (b) R. F. W. Bader, *Chem. Rev.* **1991**, *91*, 893–926. (c) R. F. W. Bader, *J. Phys. Chem. A* **1998**, *102*, 7314–7323. (d) F. Biegler-König, R. F. W. Bader and T. H. Tang, *J. Comput. Chem.* **1982**, *3*, 317–328. (e) R. F. W. Bader, *Acc. Chem. Res.* **1985**, *18*, 9–15. (f) T. H. Tang, R. F. W. Bader and P. MacDougall, *Inorg. Chem.* **1985**, *24*, 2047–2053. (g) F. Biegler-König, J. Schönbohm and D. Bayles, *J. Comput. Chem*. **2001**, *22*, 545–559. (h) F. Biegler-König and J. Schönbohm, *J. Comput. Chem.* **2002**, *23*, 1489–1494.

(S3) W. Nakanishi, T. Nakamoto, S. Hayashi, T. Sasamori and N. Tokitoh, *Chem. Eur. J.* **2007**, *13*, 255–268.

(S4) (a) W. Nakanishi, S. Hayashi and K. Narahara, *J. Phys. Chem. A*, **2009**, *113*, 10050–10057. (b) W. Nakanishi, S. Hayashi and K. Narahara, *J. Phys. Chem. A* **2008**, *112*, 13593–13599.

(S5) W. Nakanishi and S. Hayashi, *Curr. Org. Chem.* **2010**, *14*, 181–197.

(S6) (a) W. Nakanishi and S. Hayashi, *J. Phys. Chem. A* **2010**, *114*, 7423–7430. (b) W. Nakanishi, S. Hayashi, K. Matsuiwa and M. Kitamoto, *Bull. Chem. Soc. Jpn* **2012**, *85*, 1293–1305.

(S7) *Gaussian 09 (Revision D.01)*, M. J. Frisch, G. W. Trucks, H. B. Schlegel, G. E. Scuseria, M. A. Robb, J. R. Cheeseman, G. Scalmani, V. Barone, B. Mennucci, G. A. Petersson, H. Nakatsuji, M. Caricato, X. Li, H. P. Hratchian, A. F. Izmaylov, J. Bloino, G. Zheng, J. L. Sonnenberg, M. Hada, M. Ehara, K.

Toyota, R. Fukuda, J. Hasegawa, M. Ishida, T. Nakajima, Y. Honda, O. Kitao, H. Nakai, T. Vreven, J. A. Montgomery, Jr., J. E. Peralta, F. Ogliaro, M. Bearpark, J. J. Heyd, E. Brothers, K. N. Kudin, V. N. Staroverov, R. Kobayashi, J. Normand, K. Raghavachari, A. Rendell, J. C. Burant, S. S. Iyengar, J. Tomasi, M. Cossi, N. Rega, J. M. Millam, M. Klene, J. E. Knox, J. B. Cross, V. Bakken, C. Adamo, J. Jaramillo, R. Gomperts, R. E. Stratmann, O. Yazyev, A. J. Austin, R. Cammi, C. Pomelli, J. W. Ochterski, R. L. Martin, K. Morokuma, V. G. Zakrzewski, G. A. Voth, P. Salvador, J. J. Dannenberg, S. Dapprich, A. D. Daniels, Ö. Farkas, J. B. Foresman, J. V. Ortiz, J. Cioslowski and D. J. Fox, Gaussian, Inc.: Wallingford CT, 2009.

(S8) For the 6-311G(3d) basis sets, see: (a) R. C. Binning Jr. and L. A. Curtiss, *J. Comput. Chem.*, 1990, **11**, 1206-1216; (b) L. A. Curtiss, M. P. McGrath, J.-P. Blaudeau, N. E. Davis, R. C. Binning Jr. and L. Radom, *J. Chem. Phys.*, 1995, **103**, 6104-6113; (c) M. P. McGrath and L. Radom, *J. Chem. Phys.*, 1991, **94**, 511-516. For the diffuse functions (+ and ++), see: T. Clark, J. Chandrasekhar, G. W. Spitznagel and P. v. R. Schleyer, *J. Comput. Chem.*, 1983, **4**, 294-301.

(S9) D. Feller, *J. Comp. Chem.*, 1996, **17**, 1571-1586.

(S10) K. L. Schuchardt, B. T. Didier, T. Elsethagen, L. Sun, V. Gurumoorthi, J. Chase, J. Li and T. L. Windus, *J. Chem. Inf. Model.*, 2007, **47**, 1045-1052.

(S11) T. Noro, M. Sekiya and T. Koga, *Theoret. Chem. Acc.*, 2012, **131**, 1124.

(S12) (a) For inner and valence shells: T. Koga, S. Yamamoto, T. Shimazaki and H. Tatewaki, *Theor. Chem. Acc.*, 2002, **108**, 41-45; (b) For valence correlated set: M. Sekiya, T. Noro, Y. Osanai and T. Koga, *Theor. Chem. Acc.*, 2001, **106**, 297-300.

(S13) C. Møller and M. S. Plesset, *Phys. Rev.*, 1934, **46**, 618-622; J. Gauss, *J. Chem. Phys.*, 1993, **99**, 3629-3643; J. Gauss, Ber. Bunsen-Ges. *Phys. Chem.*, 1995, **99**, 1001-1008.

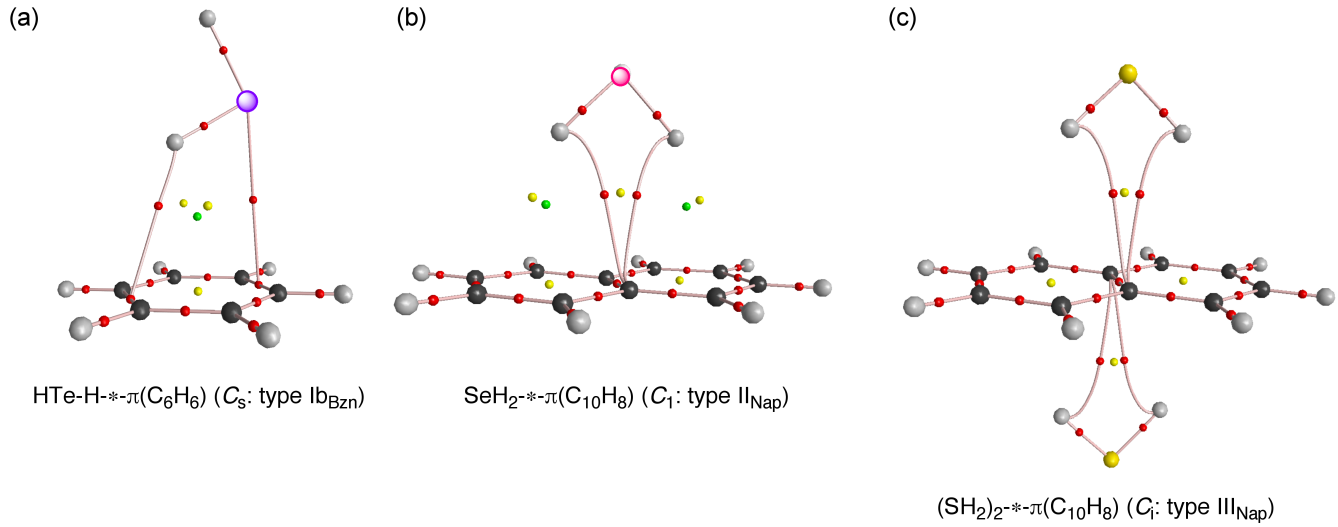

Fig. S2 Molcular graph for HTe–H-∗-π(C_6H_6) (C_s: type Ib_{Bzn}) (a), SeH_2-∗-π($C_{10}H_8$) (C_1: type II_{Nap}) (b), and $(SH_2)_2$-∗-π($C_{10}H_8$) (C_i: type III_{Nap}) (c) evaluated with MP2/BSS-F. The bond critical points (BCPs) are denoted by red dots (●), ring critical points (RCPs) by yellow dots (●) and cage critical points (CCPs) by green dots (●), together with bond paths by pink lines (-●-). Carbon atoms are in black (●) and hydrogen atoms are in gray (●) with sulfur, selenium and tellurium atoms being in yellow (●), pink (●) and purple (●), respectively.

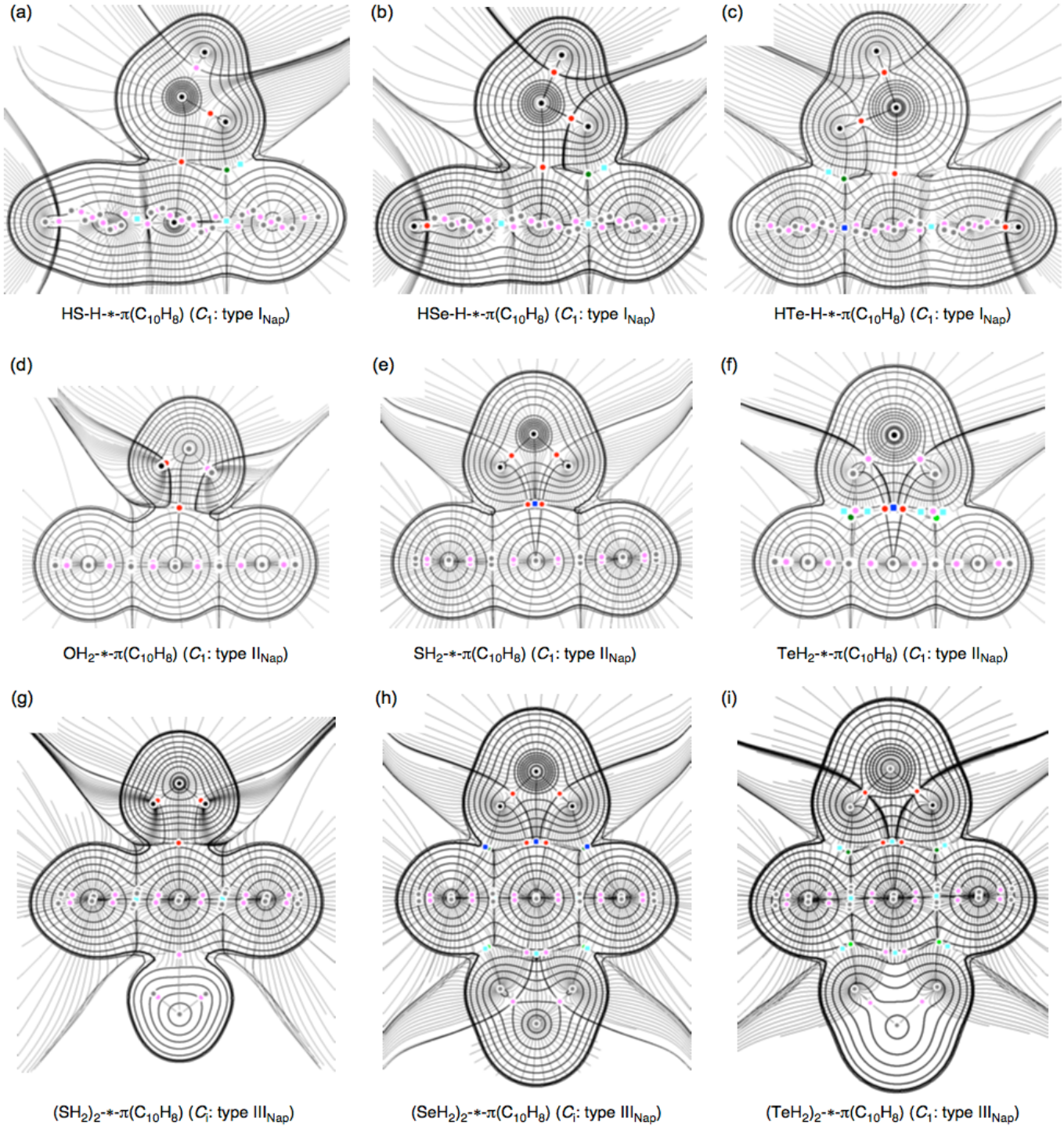

Fig. S3 Trajectory plots for HS-H-∗-π($C_{10}H_8$) (C_1: type I_{Nap}) (a), HSe-H-∗-π($C_{10}H_8$) (C_1: type I_{Nap}) (b), HTe-H-∗-π($C_{10}H_8$) (C_1: type I_{Nap}) (c), OH_2-∗-π($C_{10}H_8$) (C_1: type II_{Nap}) (d), SH_2-∗-π($C_{10}H_8$) (C_1: type II_{Nap}) (e), TeH_2-∗-π($C_{10}H_8$) (C_1: type II_{Nap}) (f), $(SH_2)_2$-∗-π($C_{10}H_8$) (C_i: type III_{Nap}) (g), $(SeH_2)_2$-∗-π($C_{10}H_8$) (C_i: type III_{Nap}) (h), and $(TeH_2)_2$-∗-π($C_{10}H_8$) (C_1: type III_{Nap}) (i), evaluated with MP2/BSS-F. Colors marks are the same as those in Fig. 3 of the text.

Table S2. Lengths of Bond Paths (r_{BP}) with Components (r_{BP-1} and r_{BP-2}) and the Corresponding Straight-line Distances (R_{SL}) in (EH_2)-∗-π($C_{10}H_8$) (E = O, S, Se and Te), Evaluated at the MP2 Levels with BSS-F[a,b]

Species (X–Y)	r_{BP-1} (Å)	r_{BP-2} (Å)	r_{BP} (Å)	R_{SL} (Å)
HB				
SH_2-∗-π (II_{Nap}: C_1)	1.5098	1.8452	3.3550	2.8791
SeH_2-∗-π (II_{Nap}: C_1)	1.4093	1.8721	3.2814	2.8966
TeH_2-∗-π (II_{Nap}: C_1)	1.6121	1.8795	3.4915	2.9706
(TeH_2-∗-π	1.1740	1.6877	2.8617	2.8290)
$(SH_2)_2$-∗-π (III_{Nap}: C_i)	1.4233	1.7308	3.1542	2.8477
$(SeH_2)_2$-∗-π (III_{Nap}: C_i)	1.4246	1.8981	3.3228	2.9037
$(TeH_2)_2$-∗-π (III_{Nap}: C_1)	1.5793	1.8755	3.4548	2.9728
EB				
HS-H-∗-π (I_{Nap}: C_1)	1.7228	1.6264	3.3492	3.3165
HSe-H-∗-π (I_{Nap}: C_1)	1.7624	1.6692	3.4315	3.3761
HTe-H-∗-π (I_{Nap}: C_1)	1.8144	1.6360	3.4504	3.3886
OH_2-∗-π (II_{Nap}: C_1)	1.7210	1.8936	3.6146	3.3637
$(OH_2)_2$-∗-π (III_{Nap}: C_1)	1.6845	1.7785	3.4630	3.3355

[a] See "Methodological Details for Calculations" of the text for BSSs. [b] See Scheme 2 of the text for r_{BP-1} and r_{BP-2}, where $r_{BP} = r_{BP-1} + r_{BP-2}$.

Optimized Structures Given by Cartesian Coordinates

MP2/BSS-F C, H: 6-311++G(d,p); S : 6-311+G(3df)
Adduct HS-H---$C_{10}H_8$
Symmetry C_1
Energy E = -783.7077414 au
Standard orientation

6	0	0.122207	-0.806170	-0.658917
6	0	0.106619	-0.581117	0.759349
6	0	1.357277	-0.713856	-1.356377
6	0	1.341020	-0.394133	1.439349
6	0	-1.113291	-0.982619	-1.339774
6	0	-1.129646	-0.671526	1.455980
6	0	2.540254	-0.504585	-0.670847
6	0	2.529628	-0.322551	0.735402
6	0	-2.306389	-1.031536	-0.639301
6	0	-2.316352	-0.857821	0.768755
1	0	1.362703	-0.849853	-2.436158
1	0	1.329906	-0.252013	2.518337
1	0	-1.103463	-1.118125	-2.419727
1	0	-1.135035	-0.532232	2.535416
1	0	3.478896	-0.441829	-1.215367
1	0	3.464932	-0.160890	1.265168
1	0	-3.242910	-1.178327	-1.171665
1	0	-3.256733	-0.906636	1.311887
16	0	-0.329160	2.575723	-0.159205
1	0	-1.038933	3.662577	-0.487511

1	0	-1.380758	1.761244	-0.314821

MP2/BSS-F C, H: 6-311++G(d,p); Se : 6-311+G(3df)
Adduct $HSe\text{-}H\text{---}C_{10}H_8$
Symmetry C_1
Energy E = -2786.1142793 au
Standard orientation

6	0	-1.175609	0.038302	0.725434
6	0	-1.148707	0.037283	-0.710857
6	0	-1.078404	1.278182	1.414262
6	0	-1.144810	1.281120	-1.399338
6	0	-1.168130	-1.205309	1.414287
6	0	-1.235215	-1.204034	-1.398519
6	0	-1.044154	2.471996	0.716242
6	0	-1.060866	2.472716	-0.701773
6	0	-1.218137	-2.399984	0.717254
6	0	-1.233575	-2.399797	-0.701437
1	0	-1.062994	1.274910	2.502498
1	0	-1.152916	1.278856	-2.487666
1	0	-1.154844	-1.202706	2.502626
1	0	-1.244962	-1.201479	-2.486917
1	0	-0.974601	3.413461	1.255143
1	0	-1.037727	3.416379	-1.240797
1	0	-1.218265	-3.343771	1.256860
1	0	-1.281185	-3.342610	-1.240602
34	0	2.154067	-0.016214	-0.012954
1	0	3.464944	-0.658935	-0.056053
1	0	1.469922	-1.305649	-0.017996

MP2/BSS-F C, H: 6-311++G(d,p); Te : 74331111/7431111/74111/21
Adduct $HTe\text{-}H\text{---}C_{10}H_8$
Symmetry C_1
Energy E = -6997.8551246 au
Standard orientation

6	0	-1.455518	0.151567	0.744995
6	0	-1.501969	0.158276	-0.691972
6	0	-1.192908	1.369567	1.430538
6	0	-1.379618	1.397312	-1.378912
6	0	-1.564662	-1.088676	1.431893
6	0	-1.751938	-1.061964	-1.377185
6	0	-1.042198	2.554305	0.731738
6	0	-1.127961	2.566826	-0.683945
6	0	-1.774605	-2.265652	0.734969
6	0	-1.853790	-2.254252	-0.681458
1	0	-1.126639	1.357068	2.516868
1	0	-1.440766	1.403464	-2.465573
1	0	-1.502343	-1.094325	2.518526
1	0	-1.812485	-1.050821	-2.463928
1	0	-0.843353	3.478574	1.268386
1	0	-1.014329	3.504085	-1.222722
1	0	-1.859008	-3.206826	1.272450
1	0	-2.026193	-3.183170	-1.219343
52	0	1.830312	-0.151350	-0.025598
1	0	3.292471	-0.910827	-0.233627
1	0	1.027417	-1.590866	-0.203905

MP2/BSS-F C, H: 6-311++G(d,p); O : 6-311+G(3df)
Adduct $OH_2\text{---}C_{10}H_8$
Symmetry C_1
Energy E = -461.1309157 au

Standard orientation

6	0	-0.075754	-0.622097	-0.554091
6	0	-0.078167	0.783401	-0.258158
6	0	-1.309550	-1.329024	-0.548439
6	0	-1.323827	1.445525	-0.077057
6	0	1.170827	-1.288878	-0.711839
6	0	1.157622	1.487277	-0.248870
6	0	-2.504509	-0.661780	-0.345728
6	0	-2.510010	0.732717	-0.086806
6	0	2.360683	-0.582935	-0.664500
6	0	2.354591	0.814384	-0.418559
1	0	-1.302582	-2.399448	-0.744184
1	0	-1.326016	2.515874	0.119867
1	0	1.173556	-2.360480	-0.901677
1	0	1.151209	2.557646	-0.052678
1	0	-3.441130	-1.213092	-0.349702
1	0	-3.453962	1.248523	0.068990
1	0	3.305856	-1.103593	-0.795379
1	0	3.293585	1.360789	-0.389297
8	0	0.536674	-0.551006	2.767676
1	0	-0.291422	-0.273264	2.363597
1	0	1.146073	-0.596436	2.023340

MP2/BSS-F C, H: 6-311++G(d,p); S : 6-311+G(3df)
Adduct SH_2---$C_{10}H_8$
Symmetry C_1
Energy E = -783.7084491 au
Standard orientation

6	0	-0.000208	-0.761556	0.720042
6	0	-0.000193	-0.721451	-0.715622
6	0	-1.242520	-0.710527	1.409628
6	0	-1.243466	-0.743551	-1.404705
6	0	1.242114	-0.711028	1.409606
6	0	1.243048	-0.744063	-1.404719
6	0	-2.437737	-0.700375	0.711822
6	0	-2.437874	-0.702007	-0.706774
6	0	2.437336	-0.701362	0.711793
6	0	2.437476	-0.703002	-0.706802
1	0	-1.239950	-0.707992	2.497966
1	0	-1.241180	-0.739593	-2.493020
1	0	1.239566	-0.708489	2.497944
1	0	1.240741	-0.740097	-2.493035
1	0	-3.380891	-0.667238	1.251273
1	0	-3.381733	-0.699244	-1.245935
1	0	3.380509	-0.668609	1.251236
1	0	3.381330	-0.700623	-1.245975
16	0	0.000777	2.815609	-0.013752
1	0	-0.964144	1.887961	0.026776
1	0	0.965448	1.887716	0.027201

MP2/BSS-F C, H: 6-311++G(d,p); Se : 6-311+G(3df)
Adduct SeH_2---$C_{10}H_8$
Symmetry C_1
Energy E = -2786.1146399 au
Standard orientation

6	0	1.275516	0.000448	0.718615
6	0	1.230610	0.000295	-0.716978
6	0	1.226356	-1.241520	1.408568
6	0	1.252684	-1.243024	-1.405737
6	0	1.225490	1.242604	1.408223
6	0	1.251805	1.243396	-1.406076

6	0	1.212870	-2.437015	0.711144
6	0	1.212103	-2.437361	-0.707448
6	0	1.211013	2.437907	0.710422
6	0	1.210306	2.437881	-0.708164
1	0	1.226109	-1.238640	2.496954
1	0	1.246866	-1.240986	-2.494095
1	0	1.225224	1.240073	2.496613
1	0	1.245868	1.241005	-2.494428
1	0	1.180581	-3.380061	1.250930
1	0	1.207617	-3.381318	-1.246504
1	0	1.178052	3.381091	1.249937
1	0	1.205092	3.381678	-1.247482
34	0	-2.377971	-0.000644	-0.005479
1	0	-1.358571	-1.044256	0.039414
1	0	-1.358332	1.041664	0.059540

MP2/BSS-F C, H: 6-311++G(d,p); Te : 74331111/7431111/74111/21
Adduct TeH_2---$C_{10}H_8$
Symmetry C_1
Energy E = -6997.8532694 au
Standard orientation

6	0	-1.590381	0.000060	0.728452
6	0	-1.676298	-0.000005	-0.705483
6	0	-1.599076	1.242820	1.417980
6	0	-1.645828	1.241970	-1.396025
6	0	-1.599136	-1.242745	1.417907
6	0	-1.645843	-1.241987	-1.396059
6	0	-1.578674	2.437435	0.719512
6	0	-1.615751	2.437469	-0.698427
6	0	-1.578767	-2.437384	0.719486
6	0	-1.615815	-2.437478	-0.698451
1	0	-1.565601	1.240198	2.505879
1	0	-1.675951	1.239731	-2.484139
1	0	-1.565662	-1.240143	2.505809
1	0	-1.675962	-1.239731	-2.484171
1	0	-1.563296	3.381349	1.258514
1	0	-1.599774	3.380732	-1.238789
1	0	-1.563420	-3.381270	1.258540
1	0	-1.599858	-3.380762	-1.238779
52	0	2.072909	-0.000013	-0.004054
1	0	0.945702	1.186849	-0.262884
1	0	0.945960	-1.187207	-0.262505

MP2/BSS-F C, H: 6-311++G(d,p); O : 6-311+G(3df)
Adduct $(OH_2)_2$---$C_{10}H_8$
Symmetry C_1
Energy E = -537.4536087 au
Standard orientation

6	0	-0.000367	-0.032537	0.717820
6	0	0.000245	0.032515	-0.717778
6	0	-1.243572	-0.004989	1.408295
6	0	-1.243199	0.027302	-1.408275
6	0	1.243141	-0.028381	1.408279
6	0	1.243503	0.006009	-1.408161
6	0	-2.438434	0.006887	0.709480
6	0	-2.438112	0.036889	-0.709514
6	0	2.438069	-0.037789	0.709549
6	0	2.438369	-0.006030	-0.709368
1	0	-1.241537	-0.029368	2.496102
1	0	-1.240672	0.051627	-2.496080
1	0	1.240603	-0.052681	2.496088

1	0	1.241495	0.030363	-2.495971
1	0	-3.381997	0.016294	1.248796
1	0	-3.381652	0.044433	-1.248901
1	0	3.381600	-0.045729	1.248938
1	0	3.381910	-0.015039	-1.248724
8	0	0.034671	3.283096	0.029275
1	0	-0.728762	2.696915	0.030725
1	0	0.783227	2.680036	-0.020145
8	0	-0.033852	-3.283011	-0.029633
1	0	0.726720	-2.695201	0.019944
1	0	-0.785342	-2.681583	-0.029866

MP2/BSS-F C, H: 6-311++G(d,p); S : 6-311+G(3df)
Adduct $(SH_2)_2$---$C_{10}H_8$
Symmetry C_i
Energy E = -1182.6087059 au
Standard orientation

6	0	-0.018319	0.000144	0.717979
6	0	0.018319	-0.000144	-0.717979
6	0	0.012019	-1.241958	1.408205
6	0	-0.008991	-1.242560	-1.407721
6	0	0.008991	1.242560	1.407721
6	0	-0.012019	1.241958	-1.408205
6	0	0.002121	-2.437497	0.710073
6	0	0.003796	-2.437796	-0.709040
6	0	-0.003796	2.437796	0.709040
6	0	-0.002121	2.437497	-0.710073
1	0	0.011006	-1.239344	2.496486
1	0	-0.007903	-1.240416	-2.496002
1	0	0.007903	1.240416	2.496002
1	0	-0.011006	1.239344	-2.496486
1	0	0.014402	-3.381025	1.249797
1	0	-0.006091	-3.381605	-1.248326
1	0	0.006091	3.381605	1.248326
1	0	-0.014402	3.381025	-1.249797
16	0	-3.551343	-0.004731	-0.013158
1	0	-2.631020	-0.969291	0.111913
1	0	-2.631559	0.959498	0.118160
16	0	3.551343	0.004731	0.013158
1	0	2.631020	0.969291	-0.111913
1	0	2.631559	-0.959498	-0.118160

MP2/BSS-F C, H: 6-311++G(d,p); Se : 6-311+G(3df)
Adduct $(SeH_2)_2$---$C_{10}H_8$
Symmetry C_i
Energy E = -5187.421015 au
Standard orientation

6	0	0.026727	0.000110	0.717780
6	0	-0.026727	-0.000110	-0.717780
6	0	0.005795	-1.241876	1.408044
6	0	-0.002451	-1.242145	-1.407853
6	0	0.002451	1.242145	1.407853
6	0	-0.005795	1.241876	-1.408044
6	0	0.011041	-2.437491	0.709692
6	0	-0.004467	-2.437659	-0.709301
6	0	0.004467	2.437659	0.709301
6	0	-0.011041	2.437491	-0.709692
1	0	0.020970	-1.239361	2.496296
1	0	-0.017630	-1.239840	-2.496106
1	0	0.017630	1.239840	2.496106
1	0	-0.020970	1.239361	-2.496296

1	0	0.007696	-3.381139	1.249475
1	0	0.001441	-3.381399	-1.248903
1	0	-0.001441	3.381399	1.248903
1	0	-0.007696	3.381139	-1.249475
34	0	-3.629661	-0.004915	0.000767
1	0	-2.611447	-1.046751	0.091524
1	0	-2.614375	1.039596	0.093606
34	0	3.629661	0.004915	-0.000767
1	0	2.611447	1.046751	-0.091524
1	0	2.614375	-1.039596	-0.093606

MP2/BSS-F C, H: 6-311++G(d,p); Te : 74331111/7431111/74111/21
Adduct $(TeH_2)_2$---$C_{10}H_8$
Symmetry C_1
Energy E = -13610.89921 au
Standard orientation

6	0	0.041461	-0.000011	0.717486
6	0	-0.041478	0.000036	-0.717349
6	0	0.029271	-1.241359	1.407906
6	0	-0.029315	-1.241339	-1.407687
6	0	0.029299	1.241419	1.407794
6	0	-0.029255	1.241401	-1.407700
6	0	0.020219	-2.437058	0.709239
6	0	-0.020315	-2.437030	-0.708926
6	0	0.020320	2.437133	0.709083
6	0	-0.020197	2.437125	-0.709072
1	0	0.064870	-1.238944	2.495855
1	0	-0.064859	-1.239041	-2.495627
1	0	0.064842	1.239119	2.495740
1	0	-0.064828	1.239005	-2.495651
1	0	0.025388	-3.380895	1.248981
1	0	-0.025474	-3.380906	-1.248607
1	0	0.025485	3.380987	1.248791
1	0	-0.025327	3.380931	-1.248872
52	0	-3.712270	0.000000	-0.000324
1	0	-2.585184	-1.186275	0.262321
1	0	-2.584967	1.185809	0.263486
52	0	3.712268	-0.000039	0.000217
1	0	2.585169	1.186241	-0.262382
1	0	2.584888	-1.185884	-0.263139